Performance Evaluation of OTFS Over Measured V2V Channels at 60 GHz

Thomas Blazek
Institute of Telecommunications
TU Wien, Vienna, Austria
thomas.blazek@tuwien.ac.at

Danilo Radovic
Institute of Telecommunications
TU Wien, Vienna, Austria
danilo.radovic@tuwien.ac.at

***Abstract*—This paper presents an analysis of the Orthogonal Time Frequency Space (OTFS) modulation scheme when applied to realistic vehicular channel situations. OTFS modulates symbols in delay-Doppler domain, hoping to exploit diversity in both. The penalty for doing this is the requirement of complex interference cancellation equalizers, as this domain incurs a strong amount of intercarrier and intersymbol interference. We conduct this analysis using measured millimeter wave vehicular channels, and we assume typical physical layer settings for a performance analysis. Our results show that there is a challenging trade-off between channel conditions that are easy to equalize and channel conditions that allow OFTS to exploit the two-dimensional diversity. In the first case we observe a good overall performance that is barely enhanced by employing OTFS. In the second case performance gain through OTFS is visible, yet with a bad overall performance.**

***Index Terms*—OTFS, mmWave, Performance Evaluation, 5G**

I. Introduction

Vehicular communications pose unique challenges to wireless communications. Due to the openness of space and high mobility of the observed channel, large delay- and Doppler spreads are to be expected [1], [2]. The current generation of Vehicle-to-Everything (V2X) communication protocols struggle with these situations due to difficult channel estimation. For future generations, different approaches have been proposed to mitigate this. IEEE 802.11bd inserts a mid-amble to enable easier channel estimation, while 5G proposes different modes to tackle with different scenarios [3].

However, many of the current approaches still base their physical layer solutions on Orthogonal Frequency Division Multiplexing (OFDM), which has its own limitations. Specifically, the format is based on a per-subcarrier one-tap equalization. While this provides simplicity in equalization of static channels, channel conditions in frequency domain are prone to fast changes, which is problematic for massive Multiple-Input Multiple-Output (MIMO) and high mobility applications. Recently, the authors of [4] have proposed a two-dimensional modulation scheme, Orthogonal Time Frequency Space (OTFS). The idea has been expanded in [5]. In this scheme, the symbols are spread out in delay- and Doppler domain, to enable exploitation of diversity in both. On the one hand, the presented approach does raise the required complexity by necessitating complex iterative decoders [6]. On the other hand, two dimensional modulations schemes have been shown to improve throughput [7], and result in relatively sparser channels [8] due to the high dimensionality of the channel. Furthermore, OTFS has been projected to better deal with highly time-variant channels [9] and scale well to massive MIMO [10]. Part of the projected gains are based on the promise that the observed channel will be sparse in the OTFS domain.

A. Our Contribution

As promising as this schemes is, careful analysis of the real-world applicability and potential has to be conducted. While OTFS is currently a strong research topic (see e.g. [11]–[13]), no analysis with real-world channels in the loop has currently been published. In this work, we evaluate the performance of OTFS when presented with actual Millimeter Wave (mmWave) measurements that represent a vehicular urban overtaking scenario. To achieve this, we take channel measurements conducted in [14], and combine them with an OTFS simulator setup. The given measurements were conducted at 60 GHz, and measured a urban scenario. The results were shown to exhibit sparse channel properties [15]. Thus, they are an ideal candidate to evaluate OTFS performance. We present a performance analysis of OTFS using an iterative Message Passing (MP) decoder presented in [6]. The performance analysis is conducted against channel sounding measurements that were done at 60 GHz for an urban overtaking scenario. We consider typical communication system transmission parameters. Our results show that it is not trivial to establish gains from an OTFS system. Parameter settings that lead to sparse delay domains are not spread out over the Doppler-domain. Conversely, settings that do diversify over Doppler see very dense delay channels. Hence, there is a trade-off between an overall sparse channel, and spreading the channel to gain from diversity. The next section presents the OTFS system model. In section III, we present the channel measurements, as well as our methodolgy to adapt them for the simulations. Section IV presents our simulation results.

II. System Model

A. OTFS Modulation

OTFS defines a delay-Doppler grid given by the lattice that consists of the cartesian product of the two dimensions [5]

$$\Lambda^{\perp} = \left\{ \left(n\Delta\tau, m\Delta\nu \right) : n \in [1, N], m \in [1, M] \right\}. \qquad (1)$$

978-1-7281-6755-8/20/$31.00 ©2020 IEEE

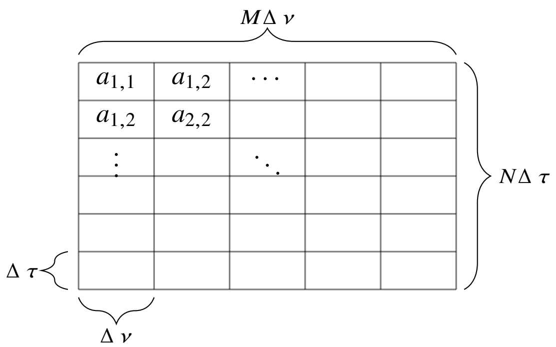

Fig. 1: Example of an OTFS grid.

Figure 1 illustrates this grid. $\Delta\tau$ defines the sampling period of the system, while $\Delta\nu$ is the lowest resolvable Doppler shift. N and M are the total number of symbols in delay and Doppler-domain respectively. OTFS requires that delay- and Doppler grid resultions have to be related via

$$\Delta\nu = \frac{1}{NM\Delta\tau}. \tag{2}$$

Each element of this grid is assigned a symbol $a_{n,m}$, e.g. from a QAM alphabet $\mathbb{A}$.

We now denote the matrix of transmit symbols $\boldsymbol{X} \in \mathbb{R}^{N\times M}$. There are multiple ways to transmit this block. One way is to transform the Doppler domain to time-domain, resulting in a data block in fast (delay) and slow (time) domain. This block can be transmitted in an appropriately interleaved fashion. Alternatively, the matrix is transformed into time-frequency domain using the *inverse symplectic discrete fourier transform* (IDSFT)

$$\boldsymbol{U}[f,t] = \frac{1}{\sqrt{NM}} \sum_{n=0}^{N-1} \sum_{m=0}^{M-1} \boldsymbol{X}[n,m] e^{-j2\pi(tm/M - fn/N)}. \tag{3}$$

f and t denote indices in frequency and (slow) time domain, and relate to physical times t' and f' via

$$t' = \frac{t}{M\Delta\nu} + T_0, \tag{4}$$

$$f' = \frac{f}{N\Delta\tau} + F_0. \tag{5}$$

F_0 and T_0 refer to the carrier frequency and start time of transmission. The symbol block $\boldsymbol{U}$ can for example be transmitted using an OFDM frontend. We now assume that the impulse responses within single subcarriers are reasonably flat. This can always be achieved by using a Cyclic Prefix (CP) in conjunction with the OFDM transmission. Then, given a block of channel transfer functions $\boldsymbol{H}[f,t]$, the received block $\boldsymbol{R}[f,t]$ equals [7]

$$\boldsymbol{R} = \boldsymbol{H} \odot \boldsymbol{U}, \tag{6}$$

where $\odot$ denotes the (element-wise) Hadamard product. The received block can be transformed back to a delay-Doppler representation $\boldsymbol{Y}[n,m]$.

TABLE I: Communication System Paramters

Parameter	Value
Center frequency	60 GHz
System bandwidth	5, 40, 120 MHz
Number of subcarriers	64
Number of Doppler samples	2, 8, 64

Alternatively, the matrix $\boldsymbol{H}$ can be represented in delay-Doppler domain as $\boldsymbol{S}_h$ [8], and the input-output relation can be described via the twisted convolution [7]

$$\boldsymbol{Y} = \boldsymbol{S}_h \star \boldsymbol{X}. \tag{7}$$

The received block can then be equalized. Due to the large amount of Intersymbol Interference (ISI) that this scheme incurs, we resort to a iterative decoding scheme. We use the Message Passing (MP) algorithm presented in [6]. The goal is to obtain the posterior estimate

$$\hat{\boldsymbol{X}} = \underset{\boldsymbol{X}\in\mathbb{A}^{N\times M}}{\arg\max}\ \Pr(\boldsymbol{X}|\boldsymbol{Y},\boldsymbol{H}). \tag{8}$$

This maximization is applied over the whole symbol matrix. In [6], this maximization is approximated by a element-by-element optimization. This element-wise optimization is updated and iterated over the whole matrix, until convergence or an iteration limit is reached.

B. *Simulation Setup*

For the performance evaluation in Section IV, we assume our simulation setup as follows. For each entry of $\boldsymbol{X}$, we draw a random symbol from a QAM alphabet. We then transmit the channel as $\boldsymbol{Y} = \boldsymbol{S}_h \star \boldsymbol{X} + \boldsymbol{N}$, where every entry of $\boldsymbol{N}$ is a zero mean complex Gaussian. The variance will be set to enforce a given Signal-to-Noise Ratio (SNR), defined as the average bit energy over the noise power E_b/N_0. In this paper, we assume perfect Channel State Information (CSI), i.e. we assume to know $\boldsymbol{H}$.

C. *System Parameters*

The system performance strongly depends on the choice of transmission parameters. Depending on the bandwidth of the system, as well as the subcarrier spacing, a communication channel may appear sparse or dense in either the delay or the Doppler domain. Hence, it is important to choose comparable parameters. We now define hypothetical parameters for a OTFS transmission system at mmWave frequencies. We define those parameters in Table I. The system has a center frequency of 60 GHz. For bandwidths, we consider 5, 40 and 120 MHz systems. On these, we use 64 subcarriers. Finally, we analyze different number of time aggregations in order to investigate the limits OFTS performance.

III. Measured V2V Channels

A. *Measurement Campaign*

A detailed description of the measurement campaign and the measurement setup is found in [14]. For ease of understanding,

TABLE II: Channel sounding measurement parameters

Parameter	Value
Center frequency	60 GHz
Subcarrier spacing	4.96 MHz
Number of subcarriers	102
Snapshot rate	129.1 μs
Delay resolution	1.96 ns
Recording time	720 ms

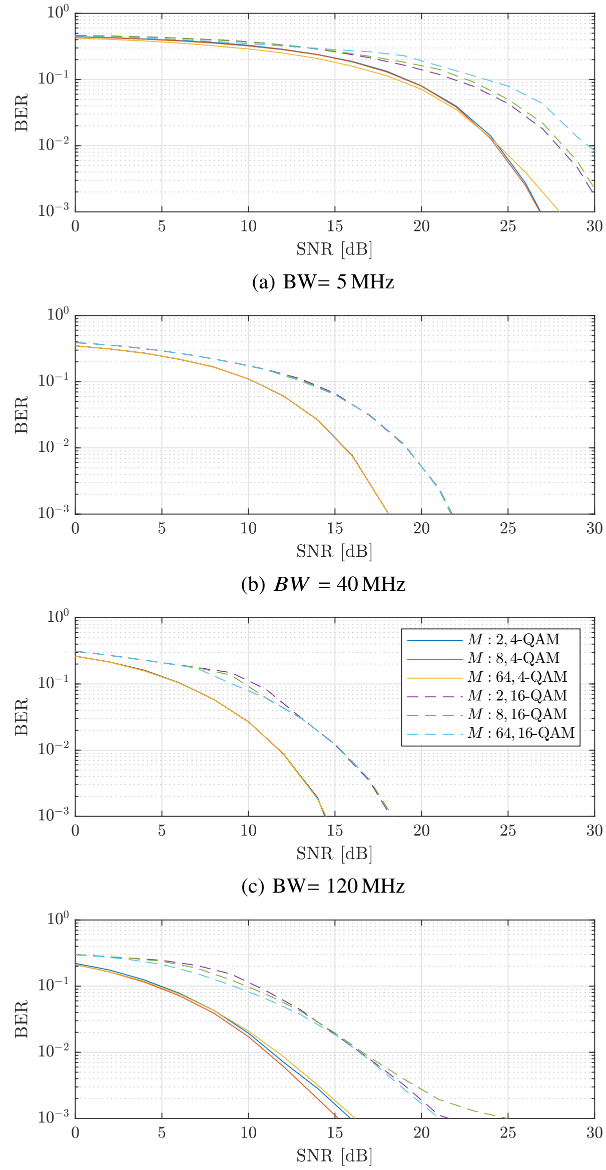

(a) BW= 5 MHz

(b) BW = 40 MHz

(c) BW= 120 MHz

(d) Synthetic channel

Fig. 2: Performance results for N=64 subcarriers. The legend is valid for all given subplots.

the key parameters of the campaign is shown in Table II, and outlined below.

The investigated scenario is close to overtaking scenarios passing a platoon. Transmitter and receiver are placed next to an urban road, and the channel is measured while cars pass by. The beginning of the measurement range is equipped with a light-barrier that indicates when a new vehicle starts to pass by, which automatically triggers a measurement. The sample rate at the receiver is 600 Msamples/s. A multitone sequence is employed with $N = 121$ carriers to approximately achieve a tone spacing of 5 MHz. Due to the anti-aliasing filter, we avoid the cut-off region and only transmit the sounding sequence at the $N_s = 101$ center tones. Thereby, an effective sounding bandwidth of 510 MHz is achieved. The output of our channel sounder is the calibrated time-variant transfer function $\boldsymbol{H}[t, f]$.

B. Delay-Doppler Interpolation

The recorded channel measurements store the results in a frequency-time grid $\boldsymbol{H}[f, t]$. However, to execute Equation (6), we have to resample in delay- and Doppler domain to match the simulation settings. The total measurement bandwidth is 500 MHz, while the subcarrier spacing is 5 MHz. We define these quantities as upper and lower bound of possible system bandwidths. To adapt the dimensions, we first ensure the new matrix $\boldsymbol{H}'$ that has the same time dimension T, but only uses a subset of f' frequency rows of $\boldsymbol{H}$. In this way, we achieve the desired bandwidth. Then, we introduce the centered, unitary Discrete Fourier Transform (DFT) matrix $\boldsymbol{F}$. We calculate a delay-time representation $\boldsymbol{G}$ via

$$\boldsymbol{G} = \begin{bmatrix} \boldsymbol{F}^{H}_{f' \times f'} \boldsymbol{H}' \\ \boldsymbol{0}^{N-f' \times T} \end{bmatrix}. \tag{9}$$

By appending $N - f'$ rows of all zeros, we ensure that the system has the correct number of subcarriers. Finally, we linearly interpolate between two consecutive snapshots, to get the desired snapshot repitition rate. We consider the linear interpolation to be of high quality, as the correlation coefficient between consecutive snapshots, defined in our case as$\rho(\boldsymbol{a}, \boldsymbol{b}) = \frac{\Re(<a,b>)}{\|a\|_2 \|b\|_2}$, is close to 0.95. Thus, the samples are highly correlated, and simple interpolation yields good performance.

IV. Performance Evaluation

We conduct the bit error performance evaluation using the channel measurements and the settings in Table I. The performance evaluation is done by comparing bit error rate (BER) at various levels of SNR. Here we use the SNR definition of expected energy per bit over noise power, SNR $= \frac{E_b}{N_0}$.

We simulate transmissions for various OTFS configurations. As channel, we use a measurement trace where a Sports Utility Vehicle (SUV) was passing by, while transmitter and receiver had line-of-sight connections. For comparison, we also use the synthetic channel described in [6]. The synthetic channel has four Rayleigh-distributed taps in delay-Doppler domain, specifically the taps have offset-indices of $\{(0, 0), (1, 1), (2, 2), (3, 3)\}$ in delay-Doppler domain, with equal power across the taps. As they are defined in terms of their indices and not absolute offsets, they are independent of the used bandwidth. Figures 2a to 2c show the achieved bit error rates

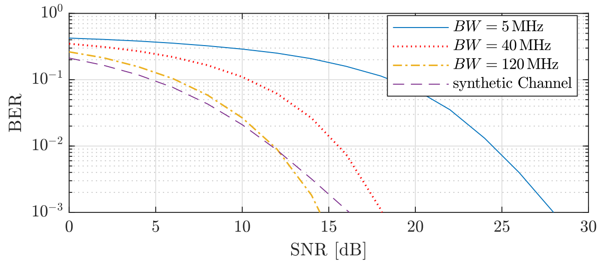

Fig. 3: Comparison of different bandwidths, 64 Doppler taps, 4-QAM.

on the measured channel with different system bandwidths. Figure 2d on the other hand shows the performance over the synthetic channel. Both bandwidths of 40 and 120 MHz show performances that are independent of the number of Doppler taps used in the OTFS configuration. This can be explained easily, as $\Delta\nu$, the lowest resolvable Doppler shift, given by Equation (2) is 9765.5 Hz in the case of $B = 40\,\mathrm{MHz}$. Meanwhile, a relative speed of 50 km/h only translates to 2778 Hz Doppler shift. Thus, the channel is completely compressed into one Doppler slot, and no diversity can be exploited without significant increment of N. For the same parameters but at 5 MHz bandwidth, the Doppler resolution becomes 1220.7 Hz. Thus, as can be seen, there is an observable gain in using OTFS. However, this comes with a severe penalty. The low bandwidth makes the channel highly dense, and the overall achievable bit error rate performs badly. In comparison, the synthetic channel demonstrates a visibly more well behaved scenario. Figure 3 shows a direct performance comparison between the different bandwidth constellations and the synthetic channel. The comparison is done with $M = 64$, and modulation scheme 4-QAM. The comparison demonstrates that the synthetic channel is a strongly optimistic estimation of the severeness of actual channels. One possible mitigation for this is to use large bandwidths and drastically increase N. However, due to the complexity of the iterative algorithm, this results in computationally prohibitively slow decoding steps.

V. Conclusions

We provide performance simulations for OTFS based on measured vehicular channels. Our results show that using OTFS can provide performance gains by exploiting two-dimensional modulation concepts. However, the used system bandwidth and Doppler resolution are linked via the modulation parameters M and N. These links remove degrees of freedom, which can stop the system from exploiting diversity in one of the considered domains. For channel estimation to benefit from OTFS, the channel has to be sparse to keep complexity low, yet spread out in both delay and Doppler domains. However, design choices that spread the channel in both domains run the risk of either increasing the denseness of the channel, or increasing the symbol dimension to computationally prohibitive sizes. On the other hand, sparse channels may become one-dimensional, removing the diversity gains. One solution to this problem may be to go for computationally more efficient receiver structures that allow denser subcarrier spacings, as well as applying, channel coding. In any case, measures have to be taken to ensure performance gains.

Acknowledgements

This work has been conducted within the DARVIS project that has received funding from the Austrian Aeronautics Research and Technology Program TAKEOFF under grant agreement No 867400.

References

[1] T. Blazek, E. Zöchmann, and C. F. Mecklenbräuker, "Model order selection for LASSO fitted millimeter wave vehicular channel data," in *Proc. of 29th Annual International Symposium on Personal, Indoor, and Mobile Radio Communications (PIMRC)*. Bologna, Italy: IEEE, Sep 2018, pp. 1–5.

[2] C. F. Mecklenbräuker, A. F. Molisch, J. Karedal, F. Tufvesson, A. Paier, L. Bernado, T. Zemen, O. Klemp, and N. Czink, "Vehicular Channel Characterization and Its Implications for Wireless System Design and Performance," *Proc. of the IEEE*, vol. 99, no. 7, pp. 1189–1212, Jul 2011.

[3] G. Naik, B. Choudhury, and J.-M. Park, "Ieee 802.11 bd & 5g nr v2x: Evolution of radio access technologies for v2x communications," *IEEE Access*, vol. 7, pp. 70 169–70 184, 2019.

[4] A. Monk, R. Hadani, M. Tsatsanis, and S. Rakib, "Otfs-orthogonal time frequency space," *arXiv preprint arXiv:1608.02993*, 2016.

[5] R. Hadani, S. Rakib, A. Molisch, C. Ibars, A. Monk, M. Tsatsanis, J. Delfeld, A. Goldsmith, and R. Calderbank, "Orthogonal time frequency space (otfs) modulation for millimeter-wave communications systems," in *2017 IEEE MTT-S International Microwave Symposium (IMS)*. IEEE, 2017, pp. 681–683.

[6] P. Raviteja, K. T. Phan, Y. Hong, and E. Viterbo, "Interference cancellation and iterative detection for orthogonal time frequency space modulation," *IEEE Transactions on Wireless Communications*, vol. 17, no. 10, pp. 6501–6515, Oct 2018.

[7] T. Zemen, M. Hofer, D. Loeschenbrand, and C. Pacher, "Iterative detection for orthogonal precoding in doubly selective channels," in *2018 IEEE 29th Annual International Symposium on Personal, Indoor and Mobile Radio Communications (PIMRC)*. IEEE, 2018, pp. 1–7.

[8] T. Blazek, H. Groll, S. Pratschner, and E. Zöchmann, "Vehicular channel characterization in orthogonal time-frequency space," in *Proceedings of the IEEE ICC 2019*, IEEE, Ed., 2019, talk: IEEE International Conference on Communications (ICC 2019), Shanghai, China; 2019-05-20 – 2019-05-24.

[9] K. Murali and A. Chockalingam, "On otfs modulation for high-doppler fading channels," in *2018 Information Theory and Applications Workshop (ITA)*. IEEE, 2018, pp. 1–10.

[10] M. K. Ramachandran and A. Chockalingam, "Mimo-otfs in high-doppler fading channels: Signal detection and channel estimation," in *2018 IEEE Global Communications Conference (GLOBECOM)*. IEEE, 2018, pp. 206–212.

[11] P. Raviteja, K. T. Phan, and Y. Hong, "Embedded pilot-aided channel estimation for otfs in delay–doppler channels," *IEEE Transactions on Vehicular Technology*, vol. 68, no. 5, pp. 4906–4917, 2019.

[12] G. D. Surabhi, M. K. Ramachandran, and A. Chockalingam, "Otfs modulation with phase noise in mmwave communications," in *2019 IEEE 89th Vehicular Technology Conference (VTC2019-Spring)*, April 2019, pp. 1–5.

[13] V. Khammammetti and S. K. Mohammed, "Otfs-based multiple-access in high doppler and delay spread wireless channels," *IEEE Wireless Communications Letters*, vol. 8, no. 2, pp. 528–531, 2018.

[14] E. Zöchmann *et al.*, "Measured delay and Doppler profiles of overtaking vehicles at 60 GHz," in *Proc. of the 12th European Conference on Antennas and Propagation (EuCAP)*, London, Great Britain, 2018, pp. 1–5.

[15] T. Blazek, E. Zöchmann, and C. Mecklenbräuker, "Millimeter wave vehicular channel emulation: A framework for balancing complexity and accuracy," *Sensors*, vol. 18, no. 11, p. 3997, 2018.